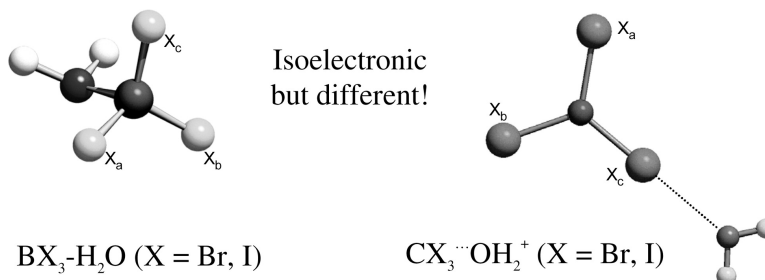


Water Adducts of BX and CX: Implications for Structure, Bonding, and Reactivity

Ingo Krossing, and Ines Raabe

J. Am. Chem. Soc., **2004**, 126 (24), 7571-7577 • DOI: 10.1021/ja030274x • Publication Date (Web): 29 May 2004

Downloaded from <http://pubs.acs.org> on March 31, 2009



More About This Article

Additional resources and features associated with this article are available within the HTML version:

- Supporting Information
- Links to the 1 articles that cite this article, as of the time of this article download
- Access to high resolution figures
- Links to articles and content related to this article
- Copyright permission to reproduce figures and/or text from this article

[View the Full Text HTML](#)

Water Adducts of BX_3 and CX_3^+ : Implications for Structure, Bonding, and Reactivity

Ingo Krossing* and Ines Raabe

Contribution from the Universität Karlsruhe, Engesserstrasse Geb. 30.45,
D-76128 Karlsruhe, Germany

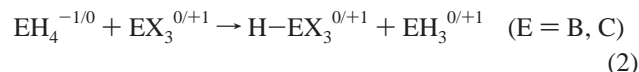
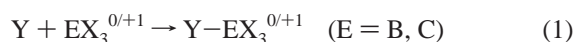
Received May 2, 2003; Revised Manuscript Received April 15, 2004; E-mail: krossing@chemie.uni-karlsruhe.de

Abstract: Good quality ab initio calculations (MP2) show that the water adducts of BX_3 and CX_3^+ have totally different structures ($X = F-I$). While all H_2O-BX_3 complexes have classical C_s symmetric structures with strong B–O bonds and additional H-bonding, the heavier CX_3^+ cations ($X = Cl-I$) form weakly bonded “non-classical” water adducts that maximize C–X π -bonding rather than C–O σ -bonding. The delocalization of the positive charge as the driving force for π -bond formation is absent in BX_3 , and therefore, π -bonding is only weak and not structure determining in H_2O-BX_3 . Since the PES of all $H_2O \rightarrow EX_3^{0/+1}$ particles ($E = B, C$) is very flat, flexible basis sets (like TZVPP) are required to rigorously characterize the adducts. In earlier calculations (*J. Am. Chem. Soc.* **1997**, *119*, 6648), classical structures were reported for all $H_2O \rightarrow EX_3^{0/+1}$ ($E = B, C$) complexes, likely resulting from the insufficient quality of the basis sets employed. By introducing a positive charge to three coordinate boron–halogen cations $Do \rightarrow BX_2^+$ ($Do = NH_3, OH_2, X-H$), also the B–X bonds shrink due to the stronger π -bonding induced by the positive charge delocalization and if compared to the respective neutral compounds like H_2N-BX_2 or BX_3 . The “non-classical” water adducts also suggest that the mechanism of organic reactions involving carbenium ion intermediates with α -bromine or -iodine substituents and a nucleophile may proceed through halogen- rather than carbon coordination.

1. Introduction

The structure and reactivity of small carbocations are of continuing interest; they are readily observed in the gas phase as well as being reactive intermediates in organic reactions.¹ Of the simple CX_3^+ cations, those with $X = Cl-I$ were characterized in solution by ¹³C NMR spectroscopy at -78 °C.² We recently prepared the first stable example of a CX_3^+ salt and reported the solid-state structure of $[Cl_3]^+[Al(OC(CF_3)_3)_4]^-$.³ Very recent results on stable CCl_3^+ and CBr_3^+ salts were also presented.⁴ This stability of the heavier CX_3^+ cations is counterintuitive and against the textbook knowledge that halogen atoms destabilize carbenium centers. These stable CX_3^+ compounds² sparked additional quantum chemical investigations^{5,6} that showed—in contrast to earlier conclusions²— Cl_3^+ to be the weakest Lewis acid of CX_3^+ ($X = H, F-I$).^{3,5} Compared to the isoelectronic BX_3 molecules,^{7,8} reversed Lewis acidities were

found based on their fluoride ion affinities³ (FIA, eq 1, $Y = F^-$) and hydride affinities.⁵ (HA, eq 2)



BX_3 and CX_3^+ are Lewis acids, and therefore, a key to the understanding of both particles was to investigate chemical reactions of both compounds, i.e., with Lewis bases. However, since only one stable Cl_3^+ salt is available, the investigations concentrated on quantum chemistry. One of the investigated Lewis bases was H_2O .⁵ The calculated water complexation energies (WCE, eq 1, $Y = H_2O$) of the CX_3^+ cations were in line with the Lewis acidities deduced from FIA and HA. The formation of $H_2O \rightarrow CX_3^+$ became less favorable for the heavier halides and was even endothermic for $X = I$. By contrast, for BX_3 , similar values for each X were calculated.⁵ Thus, the WCEs predicted BX_3 Lewis acidities that contrasted with the experimental findings.⁷ Moreover, it appeared unlikely that the WCE of the Cl_3^+ cation is positive, which suggests that the obtained minimum structure with a normal calculated C–O bond length of 159.6 pm⁵ was not the global minimum of the $H_2O \rightarrow Cl_3^+$ potential energy surface (PES). To elucidate the $H_2O \rightarrow EX_3^{0/+1}$ global minima ($E = B, C; X = H, F-I$), we

(1) (a) Olah, G. A. *J. Org. Chem.* **2001**, *66*, 5943. (b) Prakash, G. K. S., Schleyer, P. v. R., Eds. *Stable Carbocation Chemistry*; Wiley: New York, 1997.

(2) (a) Olah, G. A.; Rasul, G.; Heiliger, L.; Prakash, G. K. S. *J. Am. Chem. Soc.* **1996**, *118*, 3580. (b) Olah, G. A.; Rasul, G.; Heiliger, L.; Prakash, G. K. S. *J. Am. Chem. Soc.* **1989**, *111*, 8020.

(3) Krossing, I.; Bihlmeier, A.; Raabe, I.; Trapp, N. *Angew. Chem.* **2003**, *115*, 1569.

(4) Marcier, H. P. A.; Moran, M. D.; Schrobilgen, G. J.; Steinberg, C.; Suontamo, R. J. *J. Am. Chem. Soc.* **2004**, *126*, 5533–5548.

(5) Frenking, G.; Fau, S.; Marchand, C. M.; Grützmacher, H. *J. Am. Chem. Soc.* **1997**, *119*, 6648.

(6) Kaupp, M.; Malkina, O. L.; Malkin, V. G. *Chem. Phys. Lett.* **1997**, *265*, 55.

(7) (a) Brown, H. C.; Holmes, R. R. *J. Am. Chem. Soc.* **1956**, *78*, 2173. (b) Holmes, R. R. *J. Inorg. Nucl. Chem.* **1960**, *12*, 266.

(8) Klapötke, T. M.; Torniepoth-Oetting, I. C. *Non Metal Chemistry*; VCH: Weinheim, 1994.

recalculated several geometries of these water adducts at different levels of theory with larger DZ as well as TZ basis sets and obtained drastically different minimum structures $\text{H}_2\text{O} \rightarrow \text{CX}_3^+$ ($\text{X} = \text{Cl-I}$) from those reported earlier in this journal.⁵ Since structure and bonding of these water adducts turned out to be different for $\text{E} = \text{B}$ and C , we also performed additional calculations to analyze the influence of the positive charge in CX_3^+ in comparison to isoelectronic but neutral BX_3 . For this reason we begin with a description of the structures of $\text{EX}_3^{0/+1}$, move on to the $\text{H}_2\text{O} \rightarrow \text{EX}_3^{0/+1}$ water adducts, and finish with a series of related compounds such as $\text{X}_2\text{ENH}_2^{0/+1}$, $\text{B}_3\text{N}_3\text{H}_3\text{X}_3$ (borazine), Ph-X , $\text{X}_2\text{B-Do}^+$ ($\text{Do} = \text{NH}_3, \text{H}_2\text{O}, \text{XH}$), and BX_2^+ ($\text{X} = \text{Cl, Br, I}$) in which the presence or absence of a positive charge leads to maximum changes of structure and bonding within the E-X bonds of the particles. Then the influence of a positive charge on structure, bonding, and reactivity of these compounds is analyzed.

2. Results

2.1. Computational Details. Computations were performed with the TURBOMOLE program package.⁹ The geometries of all species were optimized at the (RI)-BP86,¹⁰ B3LYP,^{10,11} and (RI)-MP2¹² level with the SV(P)¹³ (1d polarization function) and TZVPP¹⁴ basis set (2d and 1f polarization functions). The 46 core electrons of I were replaced by a quasi relativistic effective core potential.¹⁵ Frequency calculations were performed at the same levels, and all minimum structures reported in this work are true minima without imaginary frequencies on the respective PES. To account for the basis set superposition error, reaction energies for weakly bound systems, i.e., the WCEs, were obtained by optimizing the dissociated particles, H_2O and $\text{EX}_3^{0/+1}$, in one calculation but arbitrarily separated by 1000 pm. However, the differences to the individual calculations of H_2O and $\text{EX}_3^{0/+1}$ were very small. We excluded results of population analyses from the Discussion, since different methods (NBO, AIM, or PABOON) gave very different answers for the same particles and weren't even conclusive about the sign of the partial charges residing on the individual atoms.¹⁶ Therefore, we restrict the Discussion to physical observables such as bond lengths.

2.2. Calculated Structures. Additional information for each calculated particle is deposited (one drawing, total energy,

Table 1. Calculated and Experimental Bond Lengths of $\text{EX}_3^{0/+1}$ (MP2/TZVPP)^a

	$d_{\text{exp}}(\text{C-X})$ [pm]	$d_{\text{calc}}(\text{C-X})$ [pm]	$d_{\text{exp}}(\text{B-X})$ [pm]	$d_{\text{calc}}(\text{B-X})$ [pm]
CH_3^+	—	108.6	BH_3	—
CF_3^+	—	123.3	BF_3	130.7 ¹⁷
CCl_3^+	162(1)	164.4	BCl_3	174.2 ²⁵
CBr_3^+	180.7(16) ⁴	180.8	BBR_3	189.5(1) ¹⁸
CI_3^+	201.3(9) ³	202.0	BI_3	211.8 ²⁵

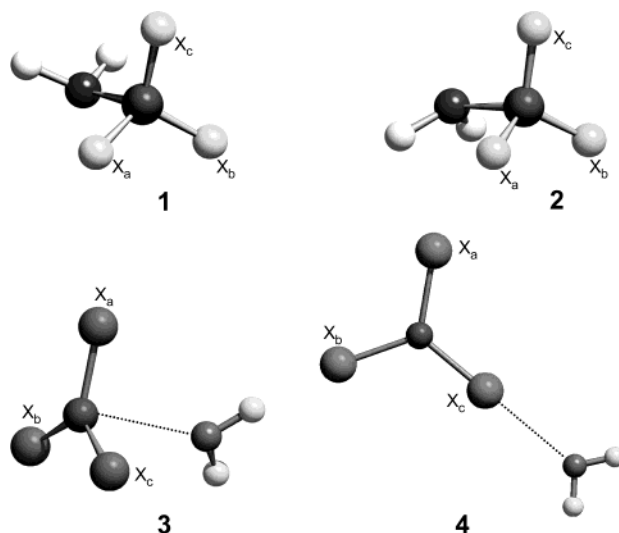


Figure 1. Minimum geometries of the water adducts $\text{H}_2\text{O} \rightarrow \text{EX}_3^{0/+1}$ ($\text{E} = \text{B, C}$; $\text{X} = \text{H, F-I}$). Covalent structures **1** and **2** vs weakly bound structures **3** and **4**. Symmetry: **1-3**: C_s , **4**: C_{2v} .

gradient, xyz orientation, structural parameters, and in part, also the vibrational frequencies).

2.2.1. Structures of Free $\text{EX}_3^{0/+1}$. To analyze the influence of the coordination of water to the $\text{EX}_3^{0/+1}$ Lewis acids ($\text{E} = \text{B, C}$; $\text{X} = \text{H, F-I}$), the free and undisturbed $\text{EX}_3^{0/+1}$ particles were investigated first. In Table 1 experimental and calculated structural parameters for $\text{EX}_3^{0/+1}$ are collected.

The E-X distances obtained by MP2/TZVPP are in very good agreement with the experimental results (within 0.1 to 2.4 pm), suggesting that conclusions drawn from these calculations hold. From Table 1 it is evident that the calculated and available experimental E-X distances in charged CX_3^+ are shorter by about 9 pm than those in isoelectronic neutral BX_3 .

2.2.2. Structures of Isomers of the Water Adducts $\text{H}_2\text{O} \rightarrow \text{EX}_3^{0/+1}$. The structures of all isomers of the $\text{H}_2\text{O} \rightarrow \text{EX}_3^{0/+1}$ adducts were optimized at the MP2/TZVPP, BP86/TZVPP,^{10,14} and B3-LYP/TZVPP^{10,11,14} levels; however, due to the better performance of MP2 to describe weak interactions, only the results based on the MP2/TZVPP calculations are discussed.

Minima on the $\text{H}_2\text{O} \rightarrow \text{EX}_3^{0/+1}$ PES. For the $\text{H}_2\text{O} \rightarrow \text{EX}_3^{0/+1}$ ($\text{E} = \text{B, C}$; $\text{X} = \text{H, F-I}$) adducts, four different minimum geometries were found (see Figure 1)¹⁹ and some minimum geometries changed with the quantum chemical method. Only the C_s symmetric structures **1** and **2** in Figure 1 were reported

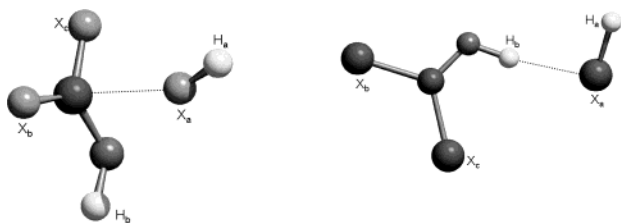
- (9) Ahlrichs, R.; Bär, M.; Häser, M.; Horn, H.; Kölmel, C. *Chem. Phys. Lett.* **1989**, *162*, 165.
 (10) (a) Slater, J. C. *Phys. Rev.* **1951**, *81*, 385. (b) Vosko, S. H.; Wilk, L.; Nusair, M. *Can. J. Phys.* **1980**, *58*, 1200. (c) Becke, A. D. *Phys. Rev. A: At., Mol., Opt. Phys.* **1988**, *38*, 3098. (d) Perdew, J. P. *Phys. Rev. B: Condens. Mater. Phys.* **1986**, *33*, 8822.
 (11) (a) Lee, C.; Yang, W.; Parr, R. G. *Phys. Rev. B: Condens. Mater. Phys.* **1988**, *37*, 785. (b) Becke, A. D. *J. Chem. Phys.* **1993**, *98*, 5648.
 (12) (a) Weigend, F.; Häser, M. *Theor. Chim. Acta* **1997**, *97*, 331. (b) Weigend, F.; Häser, M.; Patzelt, H.; Ahlrichs, R. *Chem. Phys. Lett.* **1998**, *294*, 143.
 (13) Eichkorn, K.; Treutler, O.; Oehm, H.; Häser, M.; Ahlrichs, R. *Chem. Phys. Lett.* **1995**, *242*, 652.
 (14) Schäfer, A.; Huber, C.; Ahlrichs, R. *J. Chem. Phys.* **1994**, *100*, 346.
 (15) (a) Dolg, M. Ph.D. Thesis, Stuttgart, Germany, 1989. (b) Schwerdtfeger, P.; Dolg, M.; Schwarz, W. H. E.; Bowmaker, G. A.; Boyd, P. D. W. *J. Chem. Phys.* **1989**, *91*, 1762.
 (16) Population analyses on the amount of the partial charges residing on B, C, and X are inconsistent and vary for the same particle already in the sign of the assigned charges and also change drastically with the basis sets used (NBO natural charges, AIM-, PABOON-, and Mulliken-charges at the BP86, B3-LYP, B3-PW91, and MP2 levels with increasing basis set sizes from DZ to QZ) Also, other properties such as bond orders, π -populations, etc. disagreed between the different methods. Therefore, we resisted using population analyses arguments for this report and restricted ourselves to physical observables such as bond lengths. Raabe, I.; Krossing, I. To be published.

- (17) (a) Robinson, E. A.; Johnson, S. A.; Tang, T.-H.; Gillespie, R. J. *Inorg. Chem.* **1997**, *36*, 3022. (b) Yamamoto, S.; Kuwabara, R.; Takami, N.; Kuchitsu, K. *J. Mol. Spectrosc.* **1986**, *115*, 333.
 (18) Filippini, A.; D'Angelo, P. *J. Chem. Phys.* **1998**, *109*, 5356.
 (19) For completeness, a structure type **5** was also defined (cf. figure in Supporting Information), in which one O-H bond and one of the E-X bonds are in the same plane. However, this structure does not represent the global minimum on the PES for any of the water adducts.

Table 2. Local and Global Minima of the Water Adducts $H_2O \rightarrow EX_3^{0/+1}$ ($E = B, C; X = H, F-I$) and Relative Energies (in kJ mol^{-1}) of the Different Structures at the MP2/TZVPP Level^a

geometry ^b		1		2		3		4			
$EX_3^{0/+1}$		E_{rel}	$d(E-O)$	E_{rel}	$d(E-O)$	E_{rel}	$d(E-O)$	E_{rel}	$d(E-O)$		
CH_3^+	gm	0	150.7	ts	+5.0	151.3	—	—	ts	+231.6	174.8
CF_3^+	gm	0	155.0	ts	+2.7	155.4	—	—	sp3	+127.0	256.8
CCl_3^+	—	—	—	—	—	—	gm	0	lm	+6.2	262.6
CBr_3^+	—	—	—	—	—	—	lm	+5.4	gm	0	266.4
Cl_3^+	—	—	—	—	—	—	lm	+14.6	gm	0	275.1
BH_3	gm	0	170.9	ts	+2.6	172.7	—	—	sp3	+66.6	288.9
BF_3	ts	+0.2	178.8	gm	0	179.0	—	—	—	—	—
BCl_3	gm ^c	0	166.1	lm ^c	+1.0	166.6	—	—	sp2	+31.0	312.4
BBr_3	gm ^c	0	163.8	lm ^c	+1.1	164.5	—	—	sp2	+33.7	319.7
BI_3	gm ^c	0	163.5	lm ^c	+2.6	164.4	—	—	ts	+28.7	326.5

^a Distances are given in pm. Abbreviations: gm = global minimum; lm = local minimum; ts = transition state; spn = n th order saddle point. ^b Geometries as shown in Figure 1. ^c For H_2O-BX_3 ($X = Cl-I$) structure 2 is the gm and structure 1 is a lm at the BP86/TZVPP and B3-LYP/TZVPP levels. However, the energy differences between 1 and 2 are minimal.

**Figure 2.** Calculated global minimum structures on the PES of $CH_2OF_3^+$ (left) and $CH_2OX_3^+$ ($X = Cl-I$; right) at the MP2/TZVPP level.

in the previous calculation.⁵ They are considered as being “classical” with strong E–O bonds, while structures 3 (C_s) and 4 (C_{2v}) are unexpected “non-classical” weakly bound water adducts (Structure 3 may also be viewed as classical, but with a very long and weak C–O bond (272.5 pm)). Structures 3 and 4 were obtained by using the geometries 1 and 2 as a starting point and replacing B by C^+ . Thus the energetic driving force to form the non-classical structures 3 and 4 is considerable.

Some water adducts have several minimum structures on the PES (cf. Table 2).

At the MP2 level $H_2O \rightarrow BF_3$ prefers to adopt structure 2, while 1 is a transition state albeit only 0.2 kJ mol^{-1} higher in energy. For the heavier $H_2O \rightarrow BX_3$ adducts, ($X = Cl-I$) the isomer 2 is a local minimum that is only 1.0–2.6 kJ mol^{-1} higher in energy than structure 1, whereas the halogen-bound isomers 4 are transition states or saddle points with relative energies of $\sim +29 \text{ kJ mol}^{-1}$. For the heavier $H_2O \cdots CX_3^+$ adducts, the energy differences between halogen- and carbon-bound structures are smaller. However, the carbon-bound heavier $H_2O \cdots CX_3^+$ adducts also include very long $C \cdots O$ separations exceeding 250 pm, and the halogen-coordinated isomer of $H_2O \cdots Cl_3^+$ is about 15 kJ mol^{-1} more stable than structure 3. Isomers with strong C–O bonds could not be found for the heavier CX_3^+ cations, even when starting the calculations with geometries 1 or 2. This shows that the previous calculations⁵ gave the wrong minimum structures for the heavier $H_2O \rightarrow CX_3^+$ cations ($X = Cl-I$).

As suggested by one of the reviewers, we also performed calculations on other possible isomers of $CH_2OX_3^+$ ($X = F-I$). The most favorable isomer which can be seen is $HX \cdot CX_2OH^+$ (cf. Figure 2). Two different types of structures were found. For $X = F$, the halogen is weakly bound to the carbon atom, whereas for the heavier halogens the coordination occurs through H-bonding. These species are the global minima on the PES of the $CH_2OX_3^+$ system, but since they are not water adducts, their

Table 3. Calculated Structures of the Global Minima on the PES of $CH_2OX_3^+$ ($X = F-I$) at the MP2/TZVPP Level

	F	Cl	Br	I
$d(C-X_a)$ [pm]	242.6	373.1	391.5	412.7
$d(C-X_{b,c})$ [pm]	124.5/125.4	165.2/166.5	181.7/183.0	203.1/204.5
$d(C-O)$ [pm]	124.9	126.1	126.4	127.1
$d(X_a-H_a)$ [pm]	92.6	128.2	142.0	161.0
$d(X_a-H_b)$ [pm]	299.6	194.5	210.2	228.5
angles ($X-C-X$) + ($X-C-O$) [deg]	359.9	360.0	360.0	360.0
E_{rel} [kJ/mol]	–23.6	–75.4	–51.9	–4.9

structural parameters are listed in the Results section (Table 3) but are not discussed later.

Global Minimum Structures of the Water Adducts. The global minimum structures of the water complexes of BX_3 as well as those of CH_3^+ and CF_3^+ are C_s symmetric with normal E–O bonds that range from 150.7 to 179.0 pm (Table 2). In contrast to the classical water adducts the global minimum structures of $H_2O \cdots CX_3^+$ ($X = Cl-I$) are built from trigonal planar π -bonded CX_3^+ cations and weakly interacting water molecules (266.4–275.1 pm, structures 3 and 4, Table 2). Similar weakly bound $H_2O \cdots CX_3^+$ structures ($X = Cl-I$) were also obtained by BP86 and B3LYP.

2.2.3. Structures of Related Compounds. From the preceding it followed that π -interactions appeared to be important for the heavier CX_3^+ cations (short C–X bonds, “non-classical” structures 3 and 4) but **not** for neutral isoelectronic BX_3 . Thus, we became interested in analyzing how far the positive charge in CX_3^+ may induce a stronger π -bonding if compared to neutral BX_3 . Therefore, we investigated a series of related compounds in which either (almost) no π -interaction in the E–X bond is possible ($Ph-X$, $B_3N_3H_3X_3$, H_2NBX_2) or in which a positive charge is introduced to the boron system (i.e., BX_2^+ and $Do \rightarrow BX_2^+$, $Do = NH_3$, OH_2 , XH) or strong π -donors replace the X atom in $EX_3^{0/+1}$ ($X_2E(NH_2)^{0/+1}$ and $XC(NH_2)_2^+$).²⁰ Figure 3 shows schematic drawings of the selected optimized particles.

The B–X and C–X bond lengths of the species as in Figure 3 are included in Table 6 (boron) and Table 7 (carbon) in the Discussion section; other relevant data are deposited.

3. Discussion

Although the CX_3^+ cations and the BX_3 molecules are isoelectronic species with the same D_{3h} symmetric structures,

(20) It is not suitable to include $XB(NH_2)_2$ into the discussion since the (long) B–X bond in this molecule is affected by a predissociation to the borinium salt $[(H_2N-B-NH_2)^+X^-]$.

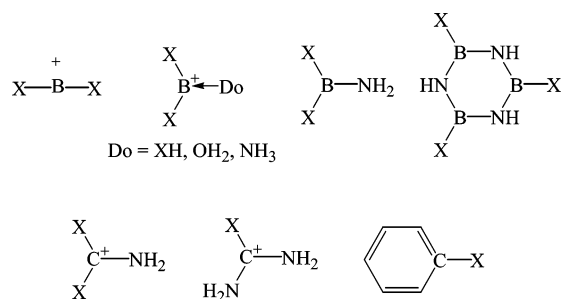


Figure 3. Schematic drawings of the additional particles optimized for $X = \text{Cl-I}$ with MP2/TZVPP. Only formal charges with no physical meaning are shown.

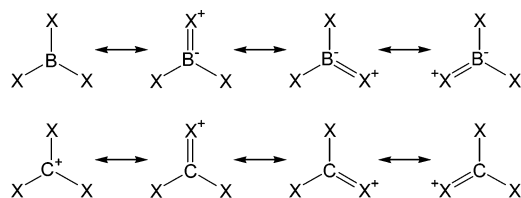


Figure 4. Possible mesomeric resonance structures for BX_3 and CX_3^+ .

their bond lengths and their chemical behavior differ considerably. In principle both BX_3 and CX_3^+ can be π -bonded by back-donation of the lone pair orbitals of the X atoms to the empty p_z orbital of the C or B atoms (Figure 4).

However, the amount of π -bonding and its influence on the structure and reactivity of $\text{EX}_3^{0/+1}$ is still under debate.²¹ One notes from Figure 4 that π -bonding leads to charge separation for BX_3 but to charge delocalization for CX_3^+ . Already this simple picture allows the assumption that π -bonding is weaker in BX_3 than it is in CX_3^+ . In other words, C^+ is a better π -acceptor than B. To shed light on the question if π -bonding is *structure determining* and thus important for the $\text{EX}_3^{0/+1}$ particles, we will first discuss the water adducts and then turn to the discussion of the related compounds as given in section 2.2.3.

3.1. H-Bonding as a Component of the Minimum Geometries of $\text{H}_2\text{O}-\text{BX}_3$. In this section we want to clarify why the WCEs of BX_3 appear **not** to follow the trend as expected from the known leveling of the Lewis acidities that increase in the order $\text{BF}_3 < \text{BCl}_3 < \text{BBr}_3 \approx \text{BI}_3$. We start with an analysis of the structures of the water adducts in Table 4 to understand the WCEs included in the same Table (MP2/TZVPP and reported⁵ values).

As may be seen from Table 4, the geometries of the $\text{H}_2\text{O} \rightarrow \text{BX}_3$ molecules are “normal” with the usual increase of the B–X bond lengths of 2.5–3.9% if compared to those of free BX_3 . The relative increase of $d(\text{B}-\text{X})$ as well as the sum of the ($\text{X}-\text{B}-\text{X}$) angles follows that expected from the Lewis acidity arguments. Also the B–O bond in $\text{H}_2\text{O} \rightarrow \text{BF}_3$, containing the weakest Lewis acid, is the longest in the series of $\text{H}_2\text{O} \rightarrow \text{BX}_3$ (179 vs 163–171 pm). Therefore, all structural parameters in $\text{H}_2\text{O} \rightarrow \text{BX}_3$ are in agreement with the known leveling of the Lewis acidity of the BX_3 molecules. Why is it then that the WCEs of BX_3 do not show this trend and remain almost

Table 4. Water Complexation Energies (WCEs) of $\text{H}_2\text{O} \rightarrow \text{BX}_3$ (values from ref 5 in parentheses), Calculated Bond Lengths, and the Sum of the X–B–X Bond Angles of $\text{H}_2\text{O} \rightarrow \text{BX}_3$ at the MP2/TZVPP Level

	BX_3			
	BF_3	BCl_3	BBr_3	BI_3
WCE [kJ mol^{-1}] ^a	40 (46)	35 (40)	41 (39)	39 (41)
$d(\text{B}-\text{O})$ [pm]	179.0	166.1	163.8	163.5
$d(\text{H}-\text{X}_{a,b})$ [pm]	263.2	281.6	291.7	307.3
$d(\text{H}-\text{X}_c)$ [pm]	308.0	282.8	293.6	309.8
$d(\text{B}-\text{X}_{a,b})$ [pm]	135.4	180.0	196.7	219.0
$d(\text{B}-\text{X}_c)$ [pm]	134.0	182.0	199.1	221.4
$d(\text{O}-\text{H})$ [pm]	96.4	97.0	97.1	97.3
stretch. B–X [%] ^b	2.5	3.7	3.9	3.8
shrink. O–H [%] ^c	0.6	1.1	1.3	1.4
$\Sigma(\text{X}-\text{B}-\text{X})$ angles [deg]	350.14	345.27	344.31	344.14

^a All values are ΔE at 0 K. ^b Compared to free BX_3 . ^c Compared to free H_2O .

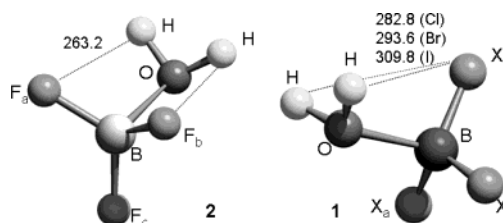


Figure 5. H-bonding in structure 1 ($\text{H}_2\text{O}-\text{BF}_3$) and structure 2 ($\text{H}_2\text{O}-\text{BX}_3$, $X = \text{Cl-I}$) at the MP2/TZVPP level.

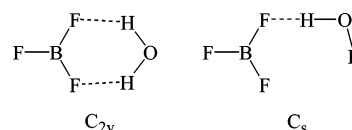


Figure 6. Geometries for the C_{2v} (left) and C_s (right) symmetric isomers of $\text{H}_2\text{O}-\text{BX}_3$ without B–O interactions.

unchanged? An analysis of Table 4 and Figure 5 shows that some structures are affected by H-bonding, most noticeably $\text{H}_2\text{O} \rightarrow \text{BF}_3$, in which two hydrogen atoms interact with two separate fluorine atoms. The H–F distance in this molecule is 263.2 pm, which is 18.6% shorter than the sum of the van der Waals radii of hydrogen and fluorine.²² Clearly this additional H-bonding makes the water adduct more stable than it would be according to the lower relative Lewis acidity of the BF_3 molecule.

This demonstrates that the higher calculated WCE of BF_3 of 40 kJ mol^{-1} is due to additional H-bonding and not due to the primarily investigated B–O bonding. To estimate the magnitude of H-bonding contributions in $\text{H}_2\text{O} \rightarrow \text{BF}_3$, we also calculated the energy of an isomer of $\text{H}_2\text{O} \rightarrow \text{BF}_3$ without any B–O interaction but with one or two H–F contacts (see Figure 6).

However, none of these structures was a minimum on the PES of this molecule; still, H-bonding stabilized both isomers by 5 (C_s) to 8 (C_{2v}) kJ mol^{-1} in comparison with the isolated monomers (MP2/TZVPP and BP86/SV(P)) while the H–F distance in the C_{2v} isomer was 254 pm and thus close to the situation in structure 2 (MP2: 263 pm). For all other $\text{H}_2\text{O} \rightarrow \text{BX}_3$ adducts an interaction as in Figure 6 only led to a minimal stabilization of at most 2 kJ mol^{-1} . Thus, the WCE of BF_3 in Table 4 of 40 kJ mol^{-1} has to be diminished by about 8 kJ mol^{-1} as a result of the additional stabilization owing to the two (weak) H-bonds (to 32 kJ mol^{-1}). Then the revised WCEs

(21) Some key references: (a) Armstrong, D. R.; Perkins, P. G. *J. Chem. Soc. (A)* **1967**, 1218. (b) Lappert, M. F.; Litzow, M. R.; Pedley, J. B.; Riley, P. N. K.; Tweedale, A. *J. Chem. Soc. (A)* **1968**, 3105. (c) Buslaev, Y. A.; Kravchenko, E. A.; Koldiz, L. *Coord. Chem. Rev.* **1987**, 82, 9. (d) Branchadell, V.; Olivia, A. *J. Am. Chem. Soc.* **1991**, 113, 4132. (e) Branchadell, V.; Olivia, A. *THEOCHEM* **1991**, 236, 75.

(22) Holleman, A. F. *Textbook of Inorganic Chemistry*, 101st ed.; Holleman-Wiberg, de Gruyter: Berlin/New York, 1995.

Table 5. Water Complexation Energies (WCEs) of $H_2O \rightarrow CX_3^+$ (values from ref 5 in parentheses), Calculated Bond Lengths, and the Sum of the X–C–X Bond Angles of $H_2O \rightarrow CX_3^+$ at the MP2/TZVPP Level^a

	CX_3^+				
	CH_3^+	CF_3^+	CCl_3^+	CBr_3^+	CI_3^+
WCE [kJ mol ⁻¹] ^b	308 (299)	168 (183)	55 (46)	52 (21)	54 (-13)
$d(C-O)$ [pm]	150.7	155.4	272.5	—	—
$d(C-X_{a,b})$ [pm]	108.1	128.9	164.4	181.4	202.6
$d(C-X_c)$ [pm]	108.2	127.8	164.2	180.4	202.6
$d(O-H)$ [pm]	97.4	97.9	96.1	96.1	96.1
stretch, C–X [%] ^c	-0.4	4.1	-0.1	0.2	0.2
shrink, O–H [%] ^d	2.0	2.1	0.3	0.3	0.3
$\Sigma(X-C-X)$ angles [deg]	338.56	341.74	359.94	360.00	360.00

^a $X_{a,b,c}$ are defined in Figure 1. ^bAll values are ΔE at 0 K. ^cCompared to free CX_3^+ . ^dCompared to free H_2O .

of the BX_3 molecules are again in line with the experimentally known Lewis acidities that follow $BF_3 < BCl_3 < BBr_3 \approx BI_3$ or WCEs of $32 < 35 < 41 \approx 39$ kJ mol⁻¹.

3.2. π -Bonding as a Structure-Determining Component of the Minimum Geometries of $H_2O \cdots CX_3^+$. In the previous work, the water adducts of the heavier CX_3^+ cations were supposed to have the structures **1** and **2** with strong C–O bonds. This was due to the use of inflexible small basis sets; our calculations with a 3-21G* basis also gave structures of these types. But already when the calculations were performed with the more flexible SV(P) or TZVPP basis sets, the weakly bound structures **3** and **4** were obtained, even when the geometry optimizations were started from the “classical” structures **1** and **2**. Therefore, the previously⁵ reported WCEs of the heavier CX_3^+ cations are wrong by a maximum of 67 kJ mol⁻¹ for CI_3^+ (Table 5, in parentheses).

For $H_2O \rightarrow CX_3^+$ ($X = H, F$) the structure **1** may be viewed as protonated methanol or trifluoromethanol. Both are known from mass spectrometry,²³ and the experimental WCE of CF_3^+ was found to be 153 ± 9 kJ mol⁻¹^{23a} in good agreement with our value of 146 kJ mol⁻¹ (both values: ΔH at 298 K²⁴). Also the experimental and the calculated values of the proton affinity of trifluoromethanol match very well: at the MP2/TZVPP level, the proton affinity is 617 kJ/mol, and the measured value is 632 ± 7 kJ/mol^{23a} (both values: ΔH at 298 K²⁴). However, the heavier $H_2O \rightarrow CX_3^+$ cations are unknown on experimental grounds, providing additional evidence for the calculated minimum structures as **not** being protonated trihalomethanols, since those certainly would have been observed in the MS. In these $H_2O \cdots CX_3^+$ ($X = Cl-I$) complexes, the CX_3^+ unit is planar (sum of bond angles $\approx 360^\circ$) and—if compared to free CX_3^+ —the C–X distances in the heavier $H_2O \cdots CX_3^+$ cations remain unchanged within 0.6 pm (see Table 5).

This planar geometry and the short C–X distances in the heavier $H_2O \cdots CX_3^+$ are chemical proof for a delocalized positive charge and for the formation of strong π -bonds. Therefore, the formation of halogen-bonded water adducts with nearly undisturbed CX_3^+ units is a result of efficient π -bonding. This indicates that for the heavier CX_3^+ cations the delocalized π -bond is more stable than the localized C–O σ -bond. Thus, in the heavier $H_2O \cdots CX_3^+$ cations the structure is determined by strong π -bonding.

3.3. Positive Charge as an Efficient Driving Force for π -Bond Formation. Why do the minimum geometries of the isoelectronic $H_2O \rightarrow EX_3^{0/+1}$ ($E = B, C$; $X = H, F - I$) species

differ so much? As shown in section 3.2 π -bonding plays an important role in CX_3^+ . What about BX_3 ? As shown in Figure 4, mesomeric structures with partial double bonds can also be formulated for BX_3 . The formation of partial π -bonds causes a positive charge on the X atoms¹⁶ if it is not overcompensated by σ -induction, and therefore, $\Delta\chi(E-X)$ is important. For the less electronegative halogens, Br and I, the transfer of the positive charge onto the halogens is easier and their ability to act as σ -acceptors is smaller. Thus, if π -bonding was important for BX_3 , at least for the heavier BX_3 molecules with $X = Br, I$, the formation of halogen-coordinated water adducts should be preferred. As shown above, this is not the case, and halogen-coordinated water adducts are transition states or saddle points at high relative energy (Table 2). The formation of partial double bonds in BX_3 would lead to a separation of the charge, which disagrees with the principle of electroneutrality. This suggests that the delocalization of the positive charge in CX_3^+ , which minimizes the overall charges, is the driving force for the formation of strong partial double bonds. Charge is absent in BX_3 , and therefore, π -interactions are weak. To support this theory, we compare calculated as well as experimental E–X bond lengths in different neutral and charged E–X species in which (i) –X is replaced by a strong π -donor such as $-NH_2$; (ii) the π -donating character of $-NH_2$ is removed by protonation to $-NH_3^+$; (iii) a positive charge is introduced to the B–X system; (iv) the C–X system bears no positive charge.

The calculated and available experimental E–X bond lengths are included with Table 6 (boron) and Table 7 (carbon).

Let us first turn to the situation of the B–X compounds in Table 6. Starting from neutral BX_3 the introduction of nitrogen lone pair orbitals as π -donors, such as the exchange of X for NH_2 ²⁰ or in the B_3N_3 borazine ring system, leads to a slight elongation of the B–X bond lengths by a maximum of 2.9 pm. This is attributed to the diminished B–X π -bonding contribution since the electron deficiency of the B atom is effectively reduced by formation of a strong dative B=N double bond²⁹ or an aromatic $6\pi B_3N_3$ ring. Thus, it may be stated that the structural effect of the B–X π -bonding in free BX_3 leads at most to a bond shortening of 2.9 pm and is therefore weak. When the π -donating character of the $-NH_2$ group in X_2B-NH_2 is destroyed by protonation and formation of $X_2B \leftarrow NH_3^+$, the B–X bonds are shortened by 6.2–7.8 pm (Figure 7).

Thus, the introduction of a positive charge to the B–X system and the absence of π -donors other than X lead to a shortening of the B–X bonds which is about 3 times stronger than the B–X bond lengthening in the BX_3 and X_2B-NH_2 couple (2.3–2.4 pm). We attribute this to the more efficient B–X π -bonding in $X_2B \leftarrow NH_3^+$ which is induced by the positive charge as a driving force. Replacing the stronger σ -donor NH_3 by weaker

- (23) (a) Chyall, L. J.; Squires, R. R. *J. Phys. Chem.* **1996**, *100*, 16435. (b) Szulejko, J. E.; McMahon, T. B. *J. Am. Chem. Soc.* **1993**, *115*, 7839.
(24) ZPE and thermal contributions to the enthalpy were included on the basis of the MP2/TZVPP frequency calculation by using the module FreeH included with TURBOMOLE.
(25) Lide, D. R.; Frederikse, H. P. R., Eds. *Handbook of Chemistry and Physics*, 76th ed.; CRC Press: Boca Raton, FL, 1995.
(26) Müller, U. *Acta Crystallogr.* **1971**, *B27*, 1997.
(27) Minkwitz, R.; Meckstroth, W.; Preut, H. *Z. Naturforsch., B: Chem. Sci.* **1993**, *48*, 19.
(28) Devillanova, F. A.; Deplano, P.; Isaia, F.; Lippolis, V.; Mercuri, M. L.; Piludu, S.; Verani, G.; Demartin, F. *Polyhedron* **1998**, *17*, 305.
(29) (a) Haaland, A. *Angew. Chem.* **1989**, *101*, 1017. (b) Lappert, M. F.; Power, P. P.; Sanger, A. R.; Srivastava, R. C. *Metal and Metalloid Amides, Synthesis, Structures, Physical and Chemical Properties*; Ellis Horwood Publishers: New York, 1980; pp 99–114 and 191–200.

Table 6. Computed (MP2/TZVPP) and Experimental²⁵ (in parentheses) B–X Distances of BX₂⁺, Do–BX₂⁺ (Do = HX, H₂O, H₃N), BX₃, Trihalogenated Borazines, and Halogenated Aminoboranes X₂B(NH₂)₂²⁰ (X = Cl–I)^a

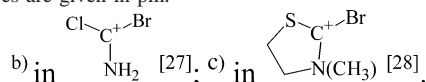
d(B–X) =	BX ₂ ⁺	HX–BX ₂ ⁺	H ₂ O–BX ₂ ⁺	H ₃ N–BX ₂ ⁺	BX ₃	H ₂ NBX ₂	B ₃ N ₃ H ₃ X ₃
X = Cl	161.5 (–)	168.1 (–) ^b	169.3 (–)	170.0 (–)	173.9 (174.2)	176.2 (–)	176.8 (176.2) ^c
X = Br	176.5 (–)	184.1 (–) ^b	185.1 (–)	185.7 (–)	189.9 (189.5)	192.3 (–)	192.8 (–)
X = I	196.9 (–)	206.0 (–) ^b	206.4 (–)	205.9 (–)	211.4 (211.8)	213.7 (–)	210.9 (–)

^a Distances are given in pm. ^b The HX–B distances are 195.3 (Cl), 209.2 (Br) and 227.0 pm (I). ^c Compare average $d_{\text{exp}}(\text{B–Cl})$ in B₃N₃Cl₆ = 176.2 pm.²⁶

Table 7. Computed (MP2/TZVPP) and Experimental²⁵ (in parentheses) C–X Distances of CX₃⁺, H₂NCX₂⁺, (H₂N)₂CX⁺, and Ph–X (X = Cl–I)^a

d(C–X)	CX ₃ ⁺	H ₂ NCX ₂ ⁺	(H ₂ N) ₂ CX ⁺	Ph–X
X = Cl	164.4 (162(1))	166.6 (169.0) ^b	168.5 (–)	173.5 (173.9) ²⁵
X = Br	180.8 (180.7 ^d)	183.0 (184.3) ^b	184.9 (184.9) ^c	189.2 (189.9) ²⁵
X = I	202.0 (201.3 ³)	204.5 (–)	206.4 (–)	209.3 (209.5) ²⁵

^a Distances are given in pm.

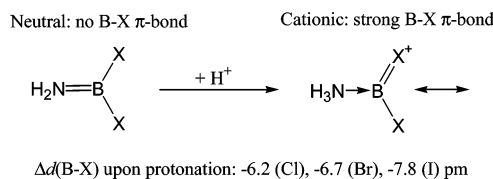
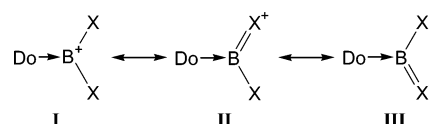


σ -donors such as OH₂ and XH leads to further, albeit small, B–X bond shortenings of at most 1.9 pm. This shows that with the weaker donors more positive charge is also left on the B atom (0th order, **I**) which is then delocalized by π -bonding (**II** and **III**), and that reduces the unfavorable localized charge formally residing on the boron atom (Figure 8).

Therefore, the driving force for π -bond formation is higher for Do \rightarrow BX₂⁺ with Do = OH₂ and XH, and their B–X bonds are further shortened if compared to X₂B \leftarrow NH₃⁺. As expected, the extreme is found for the isolated linear BX₂⁺ cation (isoelectronic with CO₂) and for which a bond shortening of 12.5–14.5 pm in comparison to that in BX₃ was found. However, the coordination number in BX₂⁺ is only 2, and the π -bond order in BX₂⁺ (between 0.5 and 1) is higher than that possible at most for BX₃ (0.33 per B–X bond).

In the carbon system in Table 7 the situation is clear; starting from the neutral Ph–X, in which an sp²-carbon resides next to a single bonded halogen atom X with (almost) no π -interaction, the introduction of a positive charge in the X_{3–x}C(NH₂)_x series leads to C–X bond shortening due to additional C–X π -bonding. The absolute shortening decreases from $x = 2$ (2.9–5.0 pm) to $x = 1$ (1.9 pm) and $x = 0$ (1.8–2.5 pm). In total, comparing Ph–X and CX₃⁺, the C–X shrinkage reaches 7.3–9.1 pm and thus is more pronounced than that in the related X₂B–NH₂/X₂B \leftarrow NH₃⁺ system (cf. 6.2–7.8 pm).

Overall, it may be stated that the effect of π -bonding is strong for CX₃⁺ but weak for BX₃. A positive charge leads to bond shortening due to π -bond formation that is more pronounced in the C–X system but is also important for the B–X system (about 85% of that of a C–X bond if comparing the related cationic CX₃⁺ and X₂B \leftarrow NH₃⁺ couple). Therefore, π -bonding is structure determining for cationic CX₃⁺ but not for neutral BX₃. For neutral BX₃, haloborazines as well as Ph–X, the positive charge as a driving force for π -bonding is absent, and therefore, the B–X bonds in neutral BX₃ (X = Cl–I) are by 9.1–9.5 pm longer than the respective C–X bonds in CX₃⁺. However, the E–X bond lengths of the related neutral couple Ph–X and trihaloborazine, which include (almost) no E–X π -bonding contribution, are comparable within 1.6–3.6 pm. This $\Delta(\text{E–X})$ is close to the intrinsic difference due to the different

**Figure 7.** π -Bond formation upon protonation of X₂B–NH₂ to X₂B \leftarrow NH₃⁺.**Figure 8.** Positive charge delocalization as the driving force for efficient π -bond formation in Do \rightarrow BX₂⁺.

covalent single bond radii of B (82 pm) and C (77 pm). Therefore, the major reason for the short C–X bonds in CX₃⁺ is strong π -bonding, while the longer B–X bonds in BX₃ are a result of the relative weakness of the structurally unimportant B–X π -bonds. Thus, the positive charge is an efficient driving force for the formation of strong π -bonds.

This conclusion underlines earlier findings that positive charge delocalization *induces* non-classical thermodynamically stable $n p_{\pi} - n p_{\pi}$ bonding ($n = 3-5$) in simple salts of heavier main group cations (i.e., E₄²⁺, E = S–Te; S₂I₄²⁺), while neutral isoelectronic species form alternative all σ -bonded classical structures. One of the extremes for this behavior is found for the P₂I₄/S₂I₄²⁺ pair.^{30,31} In neutral P₂I₄ only σ -bonding is observed; upon isoelectronic replacement of P by S⁺ the highly π -bonded S₂I₄²⁺ with a S–S bond order (b.o.) of about 2.33 and an I–I b.o. of 1.33 is formed (Figure 9).

4. Conclusions

In this contribution we analyzed the different effects that influence the structure and reactivity of the water adducts of BX₃ and CX₃⁺. To properly describe these—sometimes weak—intramolecular interactions in the water adducts, good-quality ab initio calculations (MP2) with flexible basis sets (such as TZVPP) are necessitated. We showed that the minimum structures of the heavier H₂O \rightarrow CX₃⁺ cations (X = Cl–I) reported⁵ earlier in this journal were inaccurate due to the use of insufficiently flexible basis sets. The use of very small basis sets then casts doubt on other conclusions drawn from this earlier work.⁵ Although the H₂O \rightarrow EX₃^{0/+1} species are isoelectronic, their reactivity and bonding is totally different. The BX₃ molecules form “classical” adducts with strong covalent B–O

(30) (a) Brownridge, S.; Krossing, I.; Passmore, J.; Jenkins, H. D. B.; Roobottom, H. K. *Coord. Chem. Rev.* **2000**, *197*, 397. (b) Krossing, I.; Passmore, J. *Inorg. Chem.* **1999**, *38*, 5203. (c) Cameron, T. S.; Deeth, R. J.; Dionne, I.; Du, H.; Jenkins, H. D. B.; Krossing, I.; Passmore, J.; Roobottom, H. K. *Inorg. Chem.* **2000**, *39*, 5614. (d) Murchie, M. P.; Johnson, J. P.; Passmore, J.; Sutherland, G. W.; Tajik, M.; Whidden, T. K.; White, P. S.; Grein, F. *Inorg. Chem.* **1992**, *31*, 273.

(31) Zak, Z.; Cernik, M. *Acta Crystallogr., Sect. C* **1996**, *52*, 290.

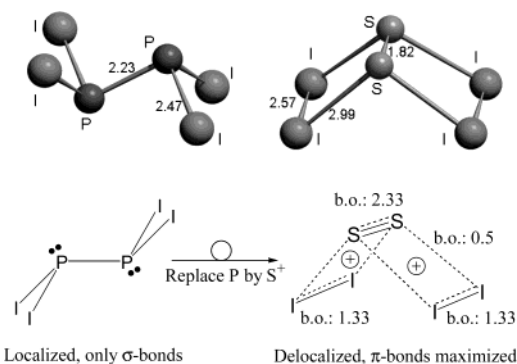


Figure 9. Structures and bond lengths of the isoelectronic species P_2I_4 (left)³¹ and $S_2I_4^{2+}$ (right, in $S_2I_4(SbF_6)_2$).³⁰ Distances given in Å.

bonds that are stabilized by additional H-bonding ($X = F$). The latter is responsible for the similarity of the WCEs of all $H_2O \rightarrow BX_3$ adducts. When the WCEs are corrected for H-bonding contributions, the WCEs follow the ordering as expected from the known Lewis acidities of the boron halides, i.e., $WCE(BF_3) < WCE(BCl_3) < WCE(BBr_3) \approx WCE(BI_3)$. The similarity of the E–X bond lengths in neutral $Ph-X$, halogenated amino-boranes or trihaloborazines, and BX_3 —in contrast to the much shortened E–X bond lengths in CX_3^+ and $Do \rightarrow BX_2^+$ —indicates that the influence of π -bonding on the structure of neutral BX_3 ($X = Cl-I$) is small and not structure determining.

The formation of weak “non-classical” water complexes of CX_3^+ ($X = Cl-I$) rather than covalent protonated trihalomethanols suggests that the delocalization of the positive charge to the less electronegative halogen atoms provides a sufficient driving force to form stable “non-classical” π -bonded ions in preference over classical all σ -bonded species. Thus, in the heavier CX_3^+ cations the bond enthalpy (BE) of a localized C–O σ bond is lower than the BE of a delocalized C–X π bond.

The “non-classical” water adducts also suggest that the mechanism of organic reactions involving carbenium ion intermediates with α -bromine or -iodine substituents and a nucleophile may proceed through halogen- rather than carbon coordination.

Acknowledgment. We thank PD Dr. H.-J. Himmel and Prof. Dr. H. Schnöckel for valuable discussions. Financial support from the *German Science Foundation DFG* and the *Fonds der Chemischen Industrie FCI* is gratefully acknowledged. Dedicated to the occasion of the 75th birthday of I.K.’s academic teacher Prof. Dr. Dr. h.c. mult. H. Nöth in München, Germany.

Supporting Information Available: Experimental details. This material is available free of charge via the Internet at <http://pubs.acs.org>.

JA030274X